

Magneto-Optics in parabolic three-dimensional quantum dots in magnetic fields of arbitrary direction

Martí Pi¹, Francesco Ancilotto², and Enrico Lipparini³

¹*Departament d'Estructura i Constituents de la Matèria,*

Facultat de Física, Universitat de Barcelona, E-08028, Spain.

²*INFN (Udr Padova and DEMOCRITOS National Simulation Center,*

Trieste, Italy) and Dipartimento di Fisica,

Università di Padova, I-35131 Padova, Italy and

³*Dipartimento di Fisica, Università di Trento,*

and INFN sezione di Trento, I-38050 Povo, Italy.

(Dated: December 12, 2018)

Abstract

We generalize the Kohn's theorem to the case of parabolic three-dimensional quantum dots in magnetic fields of arbitrary direction. We show numerically that the exact resonance frequencies in the magneto-optical absorption of these dots are reproduced by the adiabatic time-dependent local spin density approximation theory (TDLSDA). We use TDLSDA to predict spin density excitations in the dots.

PACS numbers: 71.15.Mb, 73.21.La, 73.22.Lp, 85.70.Sq

I. INTRODUCTION

Longitudinal dipole excitations in quantum dots (QD's) under applied magnetic fields have been observed in photo-absorption experiments in the far infra-red region,[1, 2] and more recently in Raman scattering experiments.[3, 4] These modes are excited by the dipole operator $\vec{D} = \sum_j \vec{r}_j$, and the resonance frequencies in the magneto-optical absorption spectrum of a QD with asymmetric parabolic confinement potential are found to be independent of the electron-electron interaction and of the number of electrons in the dot, and they coincide with the single-electron transition frequencies. This statement, known as the generalized Kohn theorem, was demonstrated some years ago by Peeters[5] for a two-dimensional QD under an external magnetic field (B) perpendicular to the plane of motion of the electrons. Peeters gave the following explicit formula for the resonance frequencies:

$$\omega_{1,2}^2 = \frac{1}{2} \left\{ (\omega_x^2 + \omega_y^2 + \omega_c^2) \pm \sqrt{(\omega_x^2 + \omega_y^2 + \omega_c^2)^2 - 4\omega_x^2\omega_y^2} \right\}, \quad (1)$$

where $\omega_c = eB/mc$ is the cyclotron frequency, and ω_x, ω_y are the confinement frequencies in the x and y directions. Time-dependent theories as time-dependent Hartree-Fock, and adiabatic time-dependent local spin density approximation (TDLSDA) fulfil the generalized Kohn theorem, [6, 7, 8] and thus any numerical implementation of these methods should reproduce the exact result of Eq. (1). Viceversa, static mean field theories like Hartree, Hartree-Fock and Kohn-Sham theories violate the theorem.[9]

In this paper we generalize the result given in Eq. (1) to the case of a parabolic three-dimensional QD in a magnetic field of arbitrary direction, and present and discuss adiabatic TDLSDA results for the dipole excitations of the same system. For density modes, the numerical calculation reproduces the exact result, and must be considered as a stringent test of our three-dimensional (3D) TDLSDA code in view of its application to study other excitation modes, like the spin dipole modes considered here, or to address the far-infrared response of more complex systems such as vertical diatomic artificial molecules.[10]

II. GENERALIZED KOHN'S THEOREM FOR 3D QUANTUM DOTS IN MAGNETIC FIELDS OF ARBITRARY DIRECTION

In the effective mass approximation, the Hamiltonian for N noninteracting electrons confined in a QD by harmonic potentials of frequencies ω_x, ω_y and ω_z in the x, y and z directions, in a constant magnetic field \vec{B} , is written as

$$H_0 = \sum_{j=1}^N h_0(j) = \sum_{j=1}^N \left\{ \frac{1}{2m} \left[\vec{p}_j - \frac{e}{c} \vec{A}_j \right]^2 + \frac{1}{2} m (\omega_x^2 x_j^2 + \omega_y^2 y_j^2 + \omega_z^2 z_j^2) + g_s^* \mu_B \vec{B} \cdot \vec{s}_j \right\}, \quad (2)$$

where $m = m^* m_e$ is the electron effective mass, \vec{A} is the vector potential which we write in the symmetric gauge as $\vec{A} = (\vec{B} \wedge \vec{r})/2$, and g_s^* is the effective gyromagnetic factor. In the numerical calculations we have used the values of m^* , dielectric constant ϵ and g^* of GaAs, namely, $m^* = 0.067$, $\epsilon = 12.4$, and $g^* = -0.44$. Without loss of generality, we write $\vec{B} = B(\sin \theta, 0, \cos \theta)$, where θ is the angle between the magnetic field and the z axis. Using hereafter effective atomic (dot) units (d.u.) $\hbar = e^2/\epsilon = m = 1$, it can be easily checked that

$$h_0 = \frac{1}{2} \vec{p}^2 + \frac{1}{2} (\omega_x^2 x^2 + \omega_y^2 y^2 + \omega_z^2 z^2) + h_m, \quad (3)$$

where

$$h_m = \frac{1}{8} \omega_c^2 [x^2 \cos^2 \theta + y^2 + z^2 \sin^2 \theta - 2xz \cos \theta \sin \theta] + \frac{1}{2} g_s^* \mu_B \eta_\sigma - \frac{i}{2} \omega_c \left[\sin \theta \left(y \frac{\partial}{\partial z} - z \frac{\partial}{\partial y} \right) + \cos \theta \left(x \frac{\partial}{\partial y} - y \frac{\partial}{\partial x} \right) \right],$$

and $\eta_\sigma = +1(-1)$ for $\sigma = \uparrow(\downarrow)$ with respect of the direction of \vec{B} . The interacting system is described by the Hamiltonian $H = H_0 + V$, where V is the electron-electron interaction

$$V = \sum_{i < j=1}^N \frac{1}{|\vec{r}_i - \vec{r}_j|}. \quad (4)$$

The single particle Hamiltonian h_0 can be exactly diagonalized:

$$h_0 = \sum_{\alpha=1}^3 \omega_\alpha \left(c_\alpha^+ c_\alpha^- + \frac{1}{2} \right), \quad (5)$$

with the creation operator c_α^+ given by

$$c_\alpha^+ = a_\alpha x + b_\alpha y + c_\alpha z + i[d_\alpha p_x + e_\alpha p_y + f_\alpha p_z]. \quad (6)$$

The operator c_α^- is the Hermitian conjugate of c_α^+ , and the coefficients $a_\alpha, \dots, f_\alpha$ in Eq. (6) are determined by solving the equation

$$[h_0, c_\alpha^+] = \omega_\alpha c_\alpha^+ , \quad (7)$$

together with the normalization condition $[c_\alpha^-, c_\alpha^+] = 1$. One gets the following homogenous system of linear equations:

$$\begin{aligned} a\omega + \frac{i}{2}b\omega_c \cos \theta + d(\omega_x^2 + \frac{1}{4}\omega_c^2 \cos^2 \theta) - \frac{1}{4}f\omega_c^2 \sin \theta \cos \theta &= 0 \\ \frac{i}{2}a\omega_c \cos \theta - b\omega - \frac{i}{2}c\omega_c \sin \theta - e(\omega_y^2 + \frac{1}{4}\omega_c^2) &= 0 \\ \frac{i}{2}b\omega_c \sin \theta - c\omega + \frac{1}{4}d\omega_c^2 \sin \theta \cos \theta - f(\omega_z^2 + \frac{1}{4}\omega_c^2 \sin^2 \theta) &= 0 \\ a + d\omega + \frac{i}{2}e\omega_c \cos \theta &= 0 \\ b - \frac{i}{2}d\omega_c \cos \theta + e\omega + \frac{i}{2}f\omega_c \sin \theta &= 0 \\ c - \frac{i}{2}e\omega_c \sin \theta + f\omega &= 0 \end{aligned} \quad (8)$$

from which the energies $\omega_1, \omega_2, \omega_3$ are obtained by solving the secular equation ($x \equiv \omega^2$):

$$\begin{aligned} x^3 - x^2(\omega_c^2 + \omega_x^2 + \omega_y^2 + \omega_z^2) \\ - x(\omega_c^2\omega_x^2 \cos^2 \theta - \omega_c^2\omega_z^2 \cos^2 \theta - \omega_y^2\omega_z^2 - \omega_x^2\omega_c^2 - \omega_x^2\omega_y^2 - \omega_x^2\omega_z^2) \\ - \omega_x^2\omega_y^2\omega_z^2 = 0 . \end{aligned} \quad (9)$$

For each energy solution ω_α , Eqs. (8) supplemented with the normalization condition

$$\text{Re} [ad^* + be^* + cf^*] = -\frac{1}{2N} , \quad (10)$$

where the $*$ indicates complex conjugation, give the coefficients $a_\alpha, \dots, f_\alpha$.

Defining $C_\alpha^+ = \sum_{j=1}^N c_{j,\alpha}^+$, it is easy to prove from Eqs. (4) and (6) that

$$[V, C_\alpha^\pm] = 0 , \quad (11)$$

which is valid not only for the Coulomb interaction but also for any V that depends only on the relative distance between any two electrons. From Eqs. (7) and (11) it follows

immediately that the Hamiltonian $H = \sum_j h_0(j) + V$ satisfies the equation of motion

$$[H, C_\alpha^\pm] = \pm \omega_\alpha C_\alpha^\pm, \quad (12)$$

which implies that if $|n\rangle$ is an eigenstate of H with energy E_n so are $C_\alpha^\pm|n\rangle$ with energies $E_n \pm \omega_\alpha$. Since in the long-wavelength limit light photoabsorption is induced by the dipole transitions, and the dipole operator can be written as a sum of C_α^+ and C_α^- operators, one recovers that dipole transitions can only occur from an eigenstate $|n\rangle$ to the eigenstates $C_\alpha^\pm|n\rangle$, and the absorption spectrum consists of three peaks of frequencies ω_1, ω_2 , and ω_3 .

As an example, we have solved the homogenous system Eqs. (8) in the case of an axially symmetric parabolic QD with $\omega_x = \omega_y = \omega_0$ by taking $\omega_0 = 4.42$ meV and $\omega_z = 18$ meV, for some values of the θ angle. The results for the three ω_α energies are reported in Fig. 1. Due to our choice of axial symmetry, at $B = 0$ the energies $\omega_{1,2}$ are degenerate and equal to ω_0 , and ω_3 coincides with ω_z . At $\theta = 0$, when \vec{B} is parallel to the symmetry axis of the dot, the solution for $\omega_{1,2}$ coincides with Peeters' expression Eq. (1), and ω_3 is B independent and equal to ω_z . At $\theta = 90^\circ$, when \vec{B} is perpendicular to the symmetry axis of the QD, it is possible to write down an analytical expression for $\omega_{2,3}$:

$$\omega_{2,3}^2 = \frac{1}{2} \left\{ (\omega_0^2 + \omega_z^2 + \omega_c^2) \pm \sqrt{(\omega_z^2 + \omega_0^2 + \omega_c^2)^2 - 4\omega_z^2\omega_0^2} \right\}, \quad (13)$$

whereas ω_1 is B independent and equal to ω_0 .

The dipole strength

$$S_{\hat{\mathbf{e}}}(\omega) = \sum_n |\langle n | \sum_j \hat{\mathbf{e}} \cdot \vec{r}_j | 0 \rangle|^2 \delta(\omega - (E_n - E_0)), \quad (14)$$

where $\hat{\mathbf{e}}$ is the polarization direction and $D_{\hat{\mathbf{e}}} = \sum_j \hat{\mathbf{e}} \cdot \vec{r}_j$ the dipole operator, can be also analytically calculated, and is different from zero only when the excitation energy $(E_n - E_0)$ is equal to the frequencies ω_α . One can show that the energy-weighted sum rule m_1

$$m_1 = \int S(\omega) \omega d\omega = \sum_n (E_n - E_0) |\langle n | D_{\hat{\mathbf{e}}} | 0 \rangle|^2 \delta(\omega - (E_n - E_0)) = \frac{N}{2}, \quad (15)$$

is exhausted by the three excited states at the energies $\omega_{1,2,3}$. The m_{-1} sum rule, related with the static polarizability, can also be worked out yielding a result that is also \vec{B} independent:

$$m_{-1} = \int S(\omega) \frac{d\omega}{\omega} = \frac{N}{2} \sum_q \frac{e_q^2}{\omega_q^2}, \quad q = x, y, z \quad (16)$$

(see also Ref. 11). By changing the values of θ and B , some strength moves from one state to another, always preserving the values of m_{-1} and m_1 .

III. TDLSDA CALCULATIONS

We now turn to our main goal which is to numerically study within TDLSDA the dipole modes both in the density and spin-density channels. As we have indicated in the Sec. I, in this approach the generalized Kohn theorem discussed previously still holds and the TDLSDA numerical results provide only a test of the 3D+time TDLSDA code. In the spin density channel the theorem does not hold, and the calculations provide an alternative prediction for this mode to that provided by the explicit evaluation of the spin-density correlation function.[6] We recall that spin dipole modes have been experimentally detected in Raman scattering experiments.[3, 4]

To obtain the dipole strength in the two channels, we study the time evolution, following an initial perturbation, of the dipole signal

$$\mathcal{D}(t) = \hat{\mathbf{e}} \cdot \langle \vec{D} \rangle , \quad (17)$$

where $\vec{D} = \sum_j \vec{r}_j$ for density dipole, and $\vec{D} = \sum_j \vec{r}_j \sigma_j^z$ for spin dipole modes, and $\langle \vec{D} \rangle$ means average over the time dependent state. This method has been used in Refs. 17, 18, 19, 20 to study charge and current modes of two-dimensional QD and quantum molecules; what follows is a generalization to the 3D case.

To calculate $\mathcal{D}(t)$, we firstly solve the static Kohn-Sham (KS) equations

$$\left[-\frac{1}{2} \left(\frac{\partial^2}{\partial x^2} + \frac{\partial^2}{\partial y^2} + \frac{\partial^2}{\partial z^2} \right) + \frac{1}{2}(\omega_x x^2 + \omega_y y^2 + \omega_z z^2) + V^H + V^{xc} + W^{xc} \eta_\sigma + h_m \right] \Psi_\sigma(x, y, z) = \epsilon_\sigma \Psi_\sigma(x, y, z) ,$$

where the expression in the square brackets is the KS Hamiltonian \mathcal{H}_{KS} . More precisely, $V^H(x, y, z)$ is the direct Coulomb potential, $V^{xc} = \delta \mathcal{E}_{xc}(n, m) / \delta n|_{gs}$, and $W^{xc} = \delta \mathcal{E}_{xc}(n, m) / \delta m|_{gs}$ are the variation of the exchange-correlation energy density $\mathcal{E}_{xc}(n, m)$ written in terms of the electron ground state (gs) density $n(x, y, z)$, and of the local spin magnetization $m(x, y, z) \equiv n^\uparrow(x, y, z) - n^\downarrow(x, y, z)$. The exchange-correlation energy has been taken from Perdew and Zunger,[12] and $\mathcal{E}_{xc}(n, m)$ has been constructed as indicated in Ref. 13. It is worth noticing that if $B \neq 0$ the single particle wave functions $\Psi_\sigma(x, y, z)$ are complex and their real and imaginary parts are coupled by h_m .

The KS equations are solved in a 3D mesh with $\Delta_x = \Delta_y = 0.51$ d.u., and $\Delta_z = 0.135$ d.u., by using 11 points formulas for the differential operators and a fast-Fourier transform to solve the Coulomb potential (for more details see Ref. 14).

Appropriate static solutions of the KS equations are then used as initial conditions for solving the time-dependent KS equations

$$i\frac{\partial}{\partial t}\psi_\sigma(\mathbf{r}, t) = \mathcal{H}_{KS}\psi_\sigma(\mathbf{r}, t), \quad (18)$$

Specifically, to describe the interaction of the system with an external dipole field the gs orbitals are slightly perturbed according to

$$\psi'_\sigma(\mathbf{r}) = U\psi_\sigma(\mathbf{r}) \quad (19)$$

with

$$U = \exp[i\lambda\hat{\mathbf{e}} \cdot \vec{r}] , \quad (20)$$

for the density dipole modes, and

$$U = \exp[i\lambda\eta_\sigma\hat{\mathbf{e}} \cdot \vec{r}] \quad (21)$$

for the spin dipole modes. Eqs. (19) and (20) give rise to an initial state in which all the electrons of the dot have a rigid velocity in an arbitrary direction $\hat{\mathbf{e}}$. In the spin dipole case, Eqs. (19) and (21) give initially to spin up and spin down electrons a rigid velocity field in opposite directions. The parameter λ is taken small enough to keep the response of the system in the linear regime.

We have solved Eqs. (18) following the method of Ref. 15. One writes

$$\psi_\sigma(\mathbf{r}, t + \delta t) - \psi_\sigma(\mathbf{r}, t - \delta t) = [e^{-i\mathcal{H}_{KS}\delta t} - e^{i\mathcal{H}_{KS}\delta t}] \psi_\sigma(\mathbf{r}, t) \quad (22)$$

and then expands the square bracket in a Taylor series:

$$\psi_\sigma(\mathbf{r}, t + \delta t) = \psi_\sigma(\mathbf{r}, t - \delta t) + 2 \sum_{j=0}^{j_{max}} (-1)^{j+1} \frac{i}{(2j+1)!} (\delta t \mathcal{H}_{KS})^{(2j+1)} \psi_\sigma(\mathbf{r}, t) . \quad (23)$$

At $t = 0$ we follow the iteration procedure of Ref. 16 up to seventh order. After the first δt step, we use Eq. (23), taking in the expansion $j_{max} = 3$. Typical δt are $\sim 2 \times 10^{-2}$ d.u. (1

d.u. is $\sim 5.55 \times 10^{-14} s$). After 15000 iterations the total energy is conserved with a relative error smaller than 10^{-11} . The dipole signal Eq. (17) is calculated every time-step.

In the linear regime the Fourier transform of the dipole signal

$$\mathcal{D}(\omega) = \int dt e^{i\omega t} \mathcal{D}(t) \quad (24)$$

is directly related to the dipole strength $S_{\hat{\mathbf{e}}}(\omega)$ Eq. (14) by

$$S_{\hat{\mathbf{e}}}(\omega) = |\mathcal{D}(\omega)|. \quad (25)$$

Hence, a frequency analysis of $\mathcal{D}(t)$ provides the absorption energies and their associate intensities.[17]

A real time simulation of the dipole evolution is shown in Fig. 2 for a $N = 6$ quantum dot for $\theta = 22.5^\circ$ and $B = 5$ T. The analysis is made for the three components of the dipole operator in the density channel, and the frequency analysis of the numerical signals providing the density dipole strength is plotted in Fig. 3 for different values of θ and B . In this figure, the energies $\omega_{1,2,3}$ yielded by the exact calculation of Sect. II are indicated with arrows. The peak energies of the TDLSDA strength are also reported with circles in Fig. 1. From these figures one may conclude that our 3D TDLSDA calculations reproduces very accurately the exact results of the previous section. From Fig. 3 one may also see how, by changing the values of θ and B , some strength moves from one mode to another.

Performing the same simulation in the spin channel we obtain the results shown in Figs. 4 and 5. Differently from the density channel, in the spin channel all the strength is mainly concentrated in one collective low energy mode. The peak energy is lower in the spin than in the density channel. This is due to the character of the TDLSDA particle-hole residual interaction, which is attractive but weak in the spin channel, and repulsive and rather strong in the density channel, shifting the TDLSDA response from the single-particle one in opposite directions.[6] Increasing the value of B , the spin mode becomes progressively softer. The TDLSDA predicts the existence of a spin instability when the energy of the spin mode goes to zero at some critical B value[6, 22]. A spin mode with this feature has been observed in GaAs quantum dots[4] using Raman spectroscopy, as well as in quantum wells[23] in a perpendicular magnetic field. In particular, in the quantum well experiment, evidence for the spin instability at some values of electron density and B has been reported.[23] The

agreement between our calculation and the experimental findings of Schüller et al. [4] in QD's is qualitatively good for low B values (see also Ref. [6]). The lack of experimental observation of collective spin states at larger B values might be considered the signature of the above mentioned instabilities. However, it cannot be excluded that Landau damping, which in this energy range is particularly strong, prevents its experimental observation. Besides, correlations beyond TDLSDA which are important for non-integer filling factors, might also quench the spin mode.

IV. SUMMARY

The dipole and spin dipole responses of a 3D quantum dot in a magnetic field of arbitrary direction have been analyzed by means of real time simulations within TDLSDA. The fragmentation of the strength due to the non circular shape of the QD and to the θ angle between the magnetic field \vec{B} and the axis perpendicular to the plane of motion of the electrons has been studied. The density dipole strengths splits in three collective states which are exactly found at the energies predicted by the generalized Kohn theorem. By changing the values of θ and of B , some strength moves from one state to another in a way which could be easily detected.

The spin dipole strength is mainly exhausted by a single, soft collective mode whose energy goes to zero as B increases, and as the direction of the applied magnetic field goes from perpendicular to parallel to the plane containing the dot. For some values of \vec{B} , TDLSDA predicts spin instabilities similar to these observed in Raman spectroscopy experiments.

A key result from our study is the circumstantial evidence that it is possible to develop a 3D code implementing TDLSDA with a magnetic field in an arbitrary direction with very high accuracy. This opens the possibility of addressing the far-infrared response of more complicated systems, such as double QD's[10] or quantum rings vertically coupled, whose description using the density-density or spin-density correlation functions[6] is prohibitive. Work along this line is now in progress.

V. ACKNOWLEDGMENTS

This work has been performed under grants BFM2002-01868 from MCyT and 2001SGR-00064 from Generalitat of Catalunya, and has been partially supported by INFM and COFIN 2001. Useful and fruitful discussions with Prof. Manuel Barranco are gratefully acknowledged.

-
- [1] Ch. Sikorski and U. Merkt, Phys. Rev. Lett. **62**, 2164 (1989).
 - [2] T. Demel, D. Heitmann, P. Grambow, and K. Ploog, Phys. Rev. Lett. **64**, 788 (1990).
 - [3] R. Strenz, U. Bockelmann, F. Hirler, G. Abstreiter, G. Böhm, and G. Weimann, Phys. Rev. Lett. **73**, 3022 (1994).
 - [4] C. Schüller, G. Biese, K. Keller, C. Steinebach, D. Heitmann, P. Grambow and K. Eberl, Phys. Rev. B **54**, R17304 (1996).
 - [5] F.M. Peeters, Phys. Rev. B **42**, 1486 (1990).
 - [6] Ll. Serra, M. Barranco, A. Emperador, M. Pi, and E. Lipparini, Phys. Rev. B **59**, 15290 (1999).
 - [7] E. Lipparini, M. Barranco, A. Emperador, M. Pi, and Ll. Serra, Phys. Rev. B **60**, 8734 (1999).
 - [8] O. Steffens and M. Suhrke, Phys. Rev. Lett. **82**, 3891 (1999).
 - [9] E. Lipparini. *Modern Many Particle Physics-Atomic Gases, Quantum Dots and Quantum Fluids*, (World Scientific, Singapore 2003).
 - [10] J.H. Oh, K.J. Chang, G. Ihm, and S.L. Lee, Phys. Rev. B **53**, R13 264 (1996); J. Hu, E. Dagotto, and A.H. MacDonald, Phys. Rev. B **54**, 8616 (1996); O. Mayrock, S.A. Mikhailov, T. Darnhofer, and U. Rössler, Phys. Rev. B **56**, 15 760 (1997); B. Partoens, A. Matulis, and F.M. Peeters, Phys. Rev. B **57**, 13 039 (1998).
 - [11] E. Lipparini, N. Barberán, M. Barranco, M. Pi, and Ll. Serra, Phys. Rev. B **56**, 12375 (1997).
 - [12] J. P. Perdew and A. Zunger, Phys. Rev. B **23**, 5048 (1981).
 - [13] M. Pi, A. Emperador, M. Barranco, F. Garcías, Phys. Rev. B **63**, 115316 (2001).
 - [14] F. Ancilotto, D.G. Austing, M. Barranco, R. Mayol, K. Muraki, M. Pi, S. Sasaki, and S. Tarucha, cond-matt/ 0207242; Phys. Rev. B in print (2003).
 - [15] R. Kosloff, J. Phys. Chem. **92** 2087 (1988).

- [16] H. Flocard, S.E. Koonin, and M.S. Weiss, Phys. Rev. **C17** 1682 (1978).
- [17] A. Puente and Ll. Serra, Phys. Rev. Lett. **83**, 3266 (1999).
- [18] Ll. Serra, A. Puente and E. Lipparini, Phys. Rev. B **60**, R13966 (1999).
- [19] M. Valín-Rodríguez, A. Puente and Ll. Serra, Eur. Phys. J. D **16**, 387 (2001).
- [20] E. Lipparini, Ll. Serra and A. Puente, Eur. Phys. J. B **27**, 409 (2002).
- [21] C.A. Ullrich and G. Vignale, Phys. Rev. B **61**, 2729 (2000).
- [22] M. Ciorga, A. Wensauer, M. Pioro-Ladriere, M. Korkusinski, J. Kyriakidis, A.S. Schrajda, and P. Hawrylak, Phys. Rev. Lett. **88**, 256804 (2002)
- [23] M. A. Eriksson, A. Pinczuk, B. S. Dennis, S. H. Simon, L. N. Pfeiffer, and K. W. West, Phys. Rev. Lett. **82**, 2163 (1999).

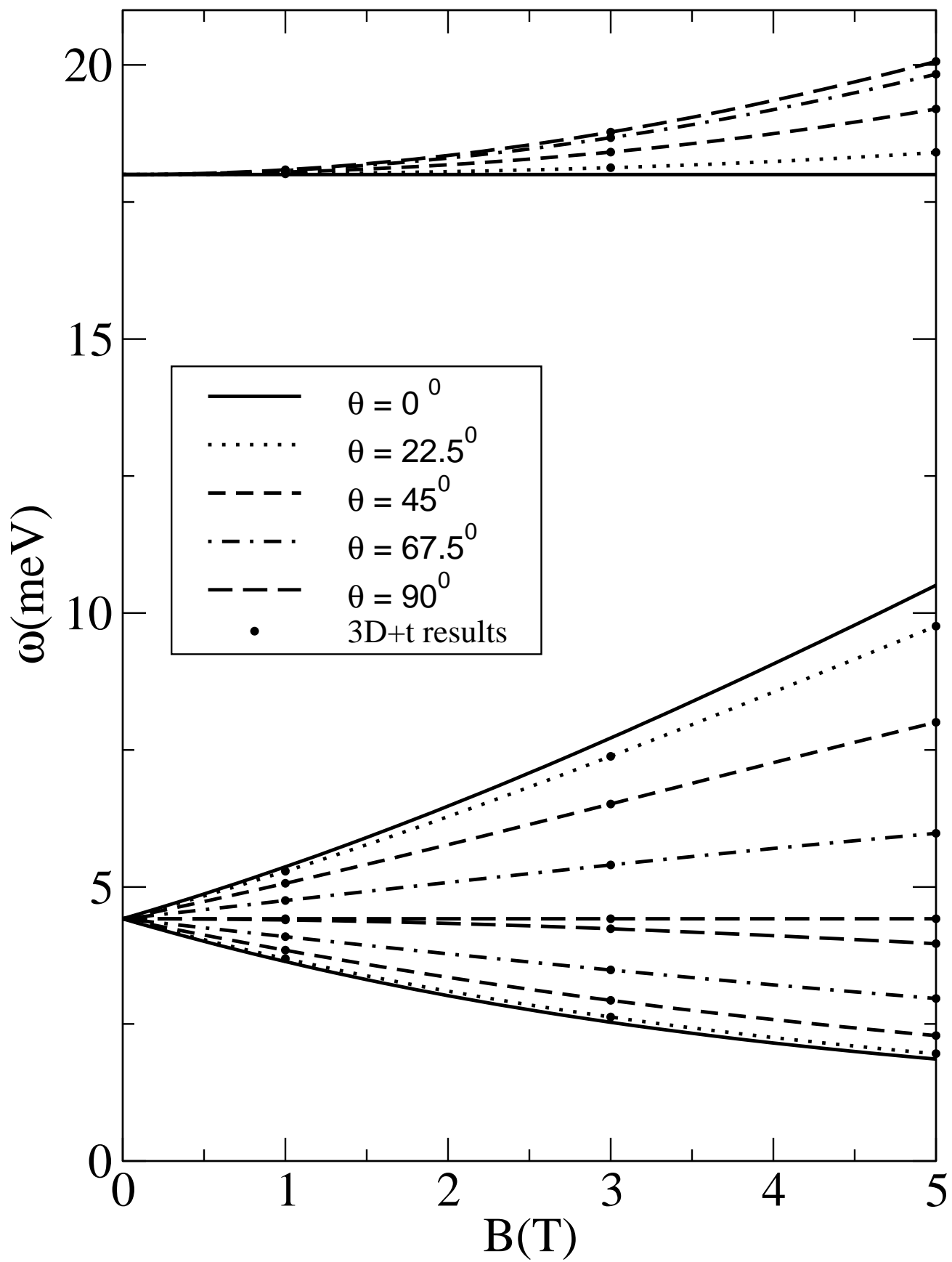
FIG. 1: Exact dispersion relation for dipole density modes. Filled circles are from TDLSDA calculations

FIG. 2: Real time evolution of the dipole density signal. Shown are the x, y and z -components of the dipole signal for $\theta = 22.5^\circ$ and $B=5\text{T}$.

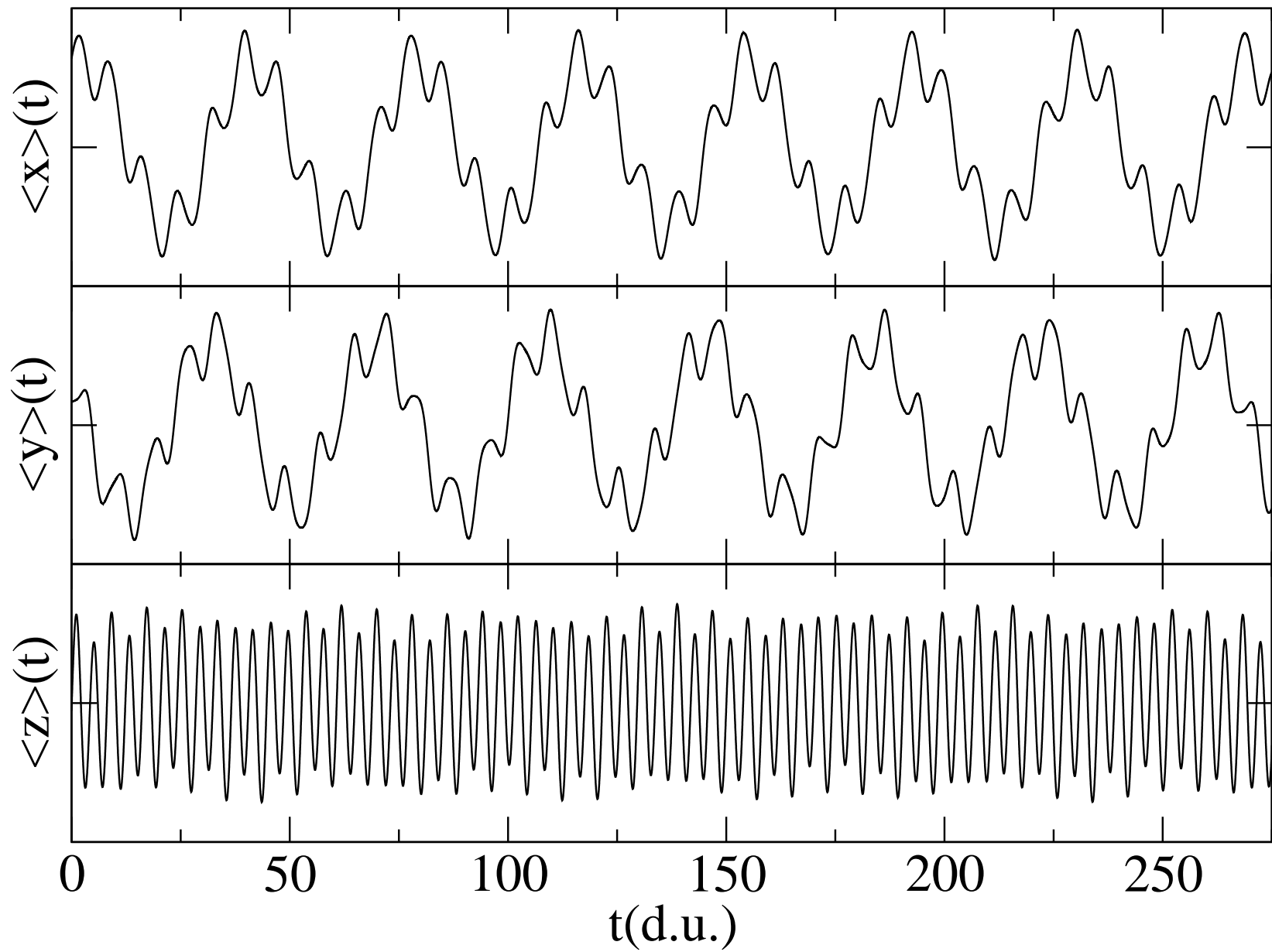
FIG. 4: Real time evolution of the dipole spin signal. Shown are the x, y and z -components of the dipole spin signal for $\theta = 67.5^\circ$ and $B=1\text{T}$.

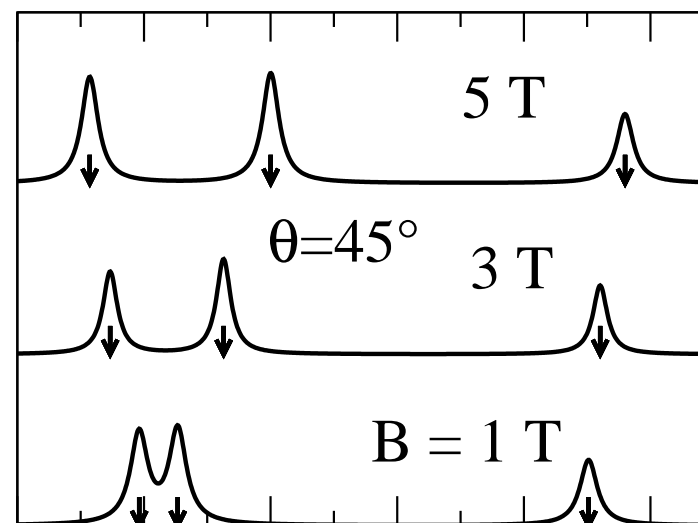
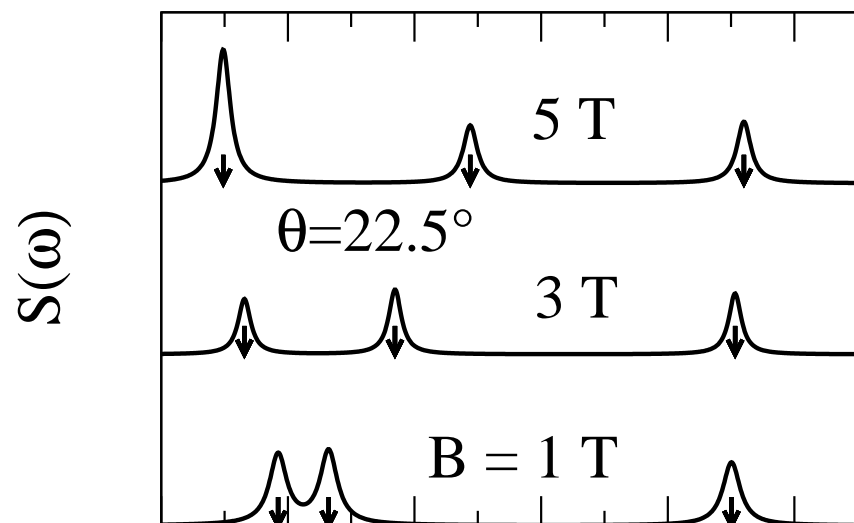
FIG. 5: Strenght function (arbitrary units) for the dipole spin response corresponding to different angles and magnetic fields.

FIG. 3: Strenght function (arbitrary units) for the dipole density response corresponding to different angles and magnetic fields.

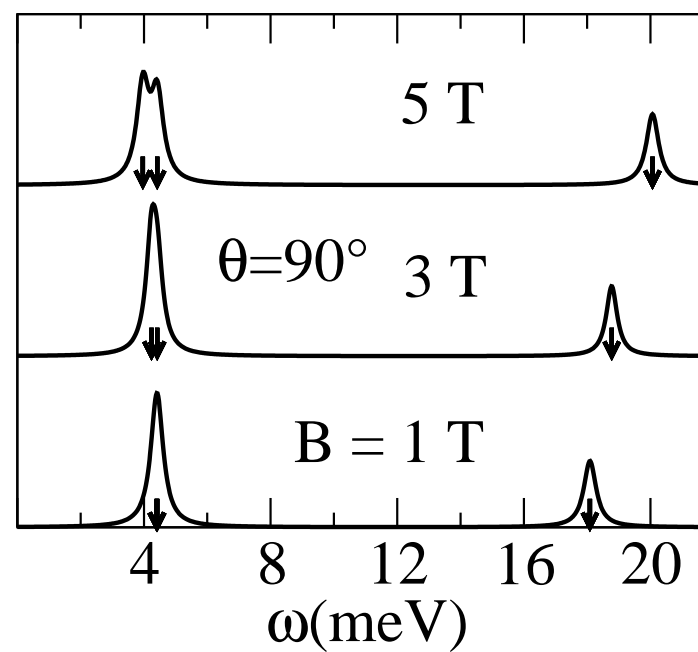
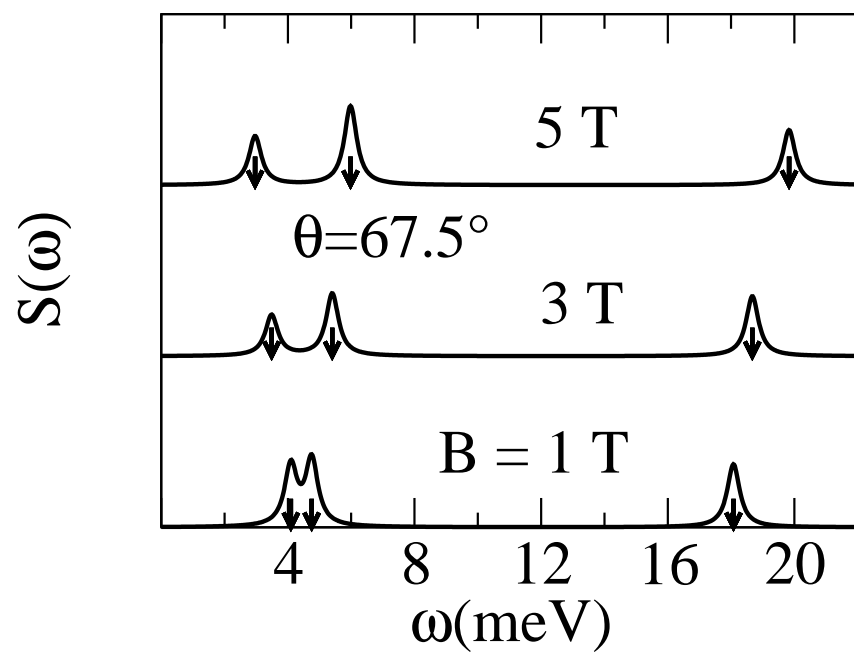


$\theta=22.5^\circ$, $B=5\text{T}$

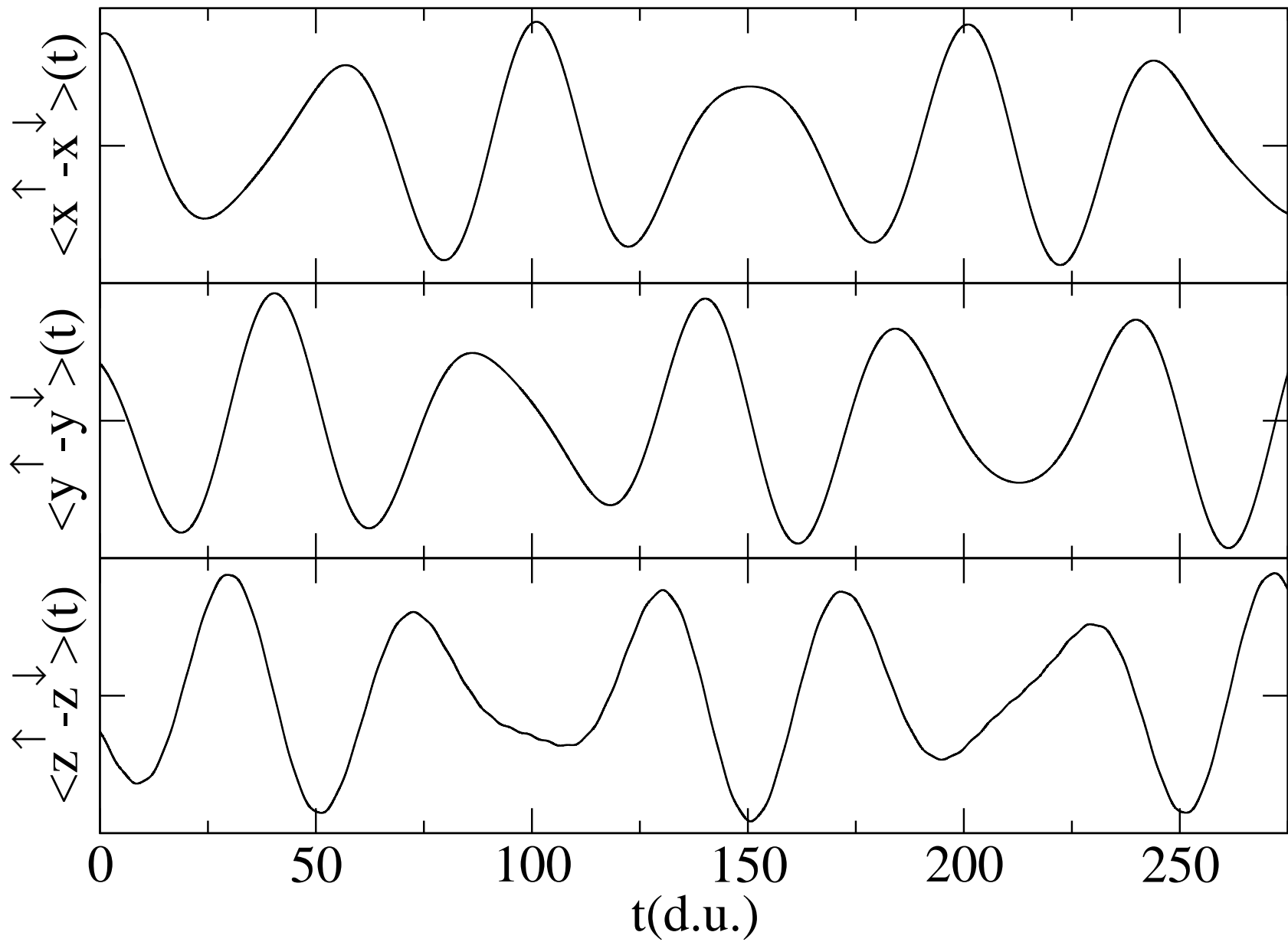


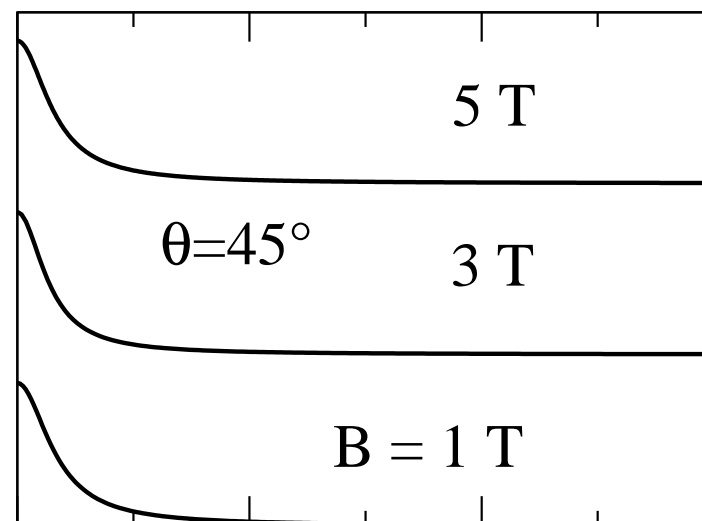
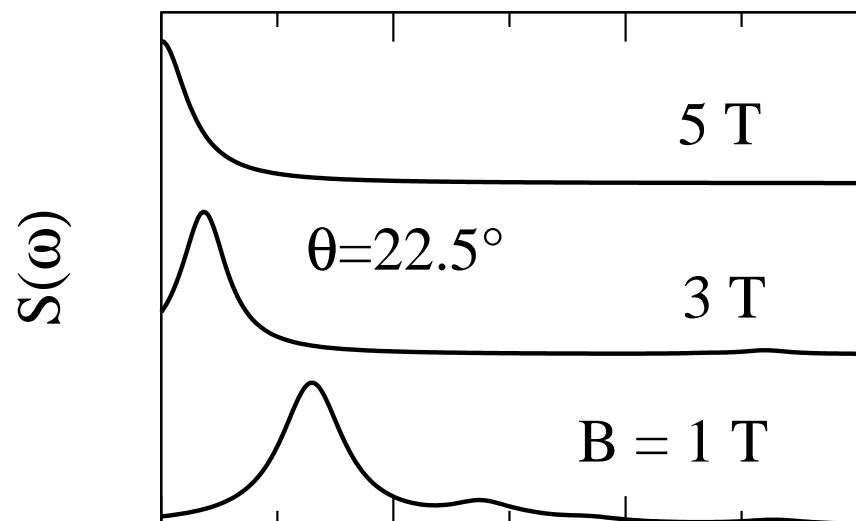


density response



$\theta=67.5^\circ$, $B=1\text{T}$





spin response

